International Journal of Modern Physics B
Vol. 19, Nos. 15, 16 & 17 (2005) 2892–2898

World Scientific
www.worldscientific.com

STUDY OF THERMAL STABILITY OF FULLERENES BY MOLECULAR DYNAMICS

WEI ZHANG, ZIJIAN XU and ZHIYUAN ZHU

Shanghai Institute of Applied Physics, Shanghai, 201800, P. R. China
Graduate School of the Chinese Academy of Sciences, Beijing, 100039, P. R. China

Received 4 September 2004

The thermal stability of fullerene C_{20}, C_{26}, C_{36} and C_{60} is studied using Molecular Dynamics (MD) simulation based on Brenner potential in this work. Lindemann's relative root-mean-square (rms) bond-length fluctuation is used to monitor the behavior of the structural and thermal properties. The results show that the rms bond-length fluctuation becomes scattered points at relative high tempereture, which is caused by different isomerization transitions. Larger fullerenes are found to be more stable than small ones. The results are compared with those from MD simulation based on TLHT potential. Mechanic stability of fullerene C_{20} is also studied.

1. Introduction

Since the synthesis of macroscopic quantity of C_{60} and C_{70}, the fullerene family has stimulated enormous interests in their chemical and physical properties[1]. Particular emphasis has been placed on their electrical transport, optical and chemical properties. Although under appropriate experimental conditions one can produce macroscopic quantities of fullerene molecules, their microscopic formation mechanism is still a very puzzling question. Studying zero-temperature properties of fullerenes is not sufficient for explaining their formation. Since some of the fullerenes can be synthesized in high temperature processes, such as arc burning or laser vaporization of graphite, thermal dynamics may play an important role in the formation. Study of the thermal properties may be helpful to explain the formation mechanism. Molecular Dynamics (MD) simulation can be used to study these properties. In the study of thermal properties such as melting transition, large thermal fluctuations are present, and therefore much longer simulation time is required. The limitation of first-principle MD simulations based on density functional theory is related the relatively short simulation time because of the large computational effort involved in the simulations. At the same time, MD simulation based on many-body model potential has its advantage over first-principle MD simulation because it allow the extension of simulation time greatly. Several many-body potentials have been proposed for the carbon covalent systems, such as TLHT potential[2], Tersoff potential[3],

Brenner potential[4], EDIP potential[5] and so on. In previous work[6,7,8], thermal stability of C_{20}, C_{36} and C_{60} is studied using MD simulation based on TLHT potential and Tersoff potential. In this paper we use MD based on Brenner potential to study the thermal stability of fullerenes.

2. Interaction Potential and Simulation Procedure

We performed constant-energy MD over a wide range of fullerene energies corresponding to temperatures ranging from 0K to 5000K, when the thermal decomposition of the fullerenes happens. The energies of fullerenes are increased by simply scaling up the atomic velocities during a step of the simulation. Brenner potential is used to mimic the short-range covalent interaction between carbon atoms in the fullerenes. The long-range interaction of carbon atoms is simulated by a Lennard-Jones-like potential proposed by Girifalco[9], which has the form

$$e(r) = -A/r^6 + B/r^{12}. \tag{1}$$

where r is the distance between two atoms, and $A = 20eV \cdot \mathring{A}^6$, $B = 3.4856 \times 10^4 eV \cdot \mathring{A}^{12}$.

Within this MD, Newton's equations of motion are solved for each atom in the fullerenes using a three-order Gear predictor-corrector algorithm. The time step is 0.2fs. For each temperature of fullerene there are 2×10^5 time steps in the simulation.

Fullerenes' structures are optimized using a thermal quenching procedure. At each simulation for a temperature, the initial structure is the same fullerene structure optimized. This is different from refs.[6,7], in which the initial structure at a higher temperature is the last structure in the previous simulation at a lower temperature. Initial atomic velocities are sampled according to Maxwell's distribution. The energy of translation of the center of mass and the rotation around the center of the fullerenes are not be included in the fullerene temperature calculation. As an initial condition, they are both removed by subtracting the translational velocity of the center of mass and rotational velocities around the center of mass from atomic velocities.

The behavior of the structural and thermal properties during the simulation is monitored by calculating the temperature and the fluctuation of root-mean-square (rms) bond length. It is defined as

$$\delta = \frac{2}{N(N-1)} \sum \frac{|\langle r_{ij}^2 \rangle - \langle r_{ij} \rangle^2|}{\langle r_{ij} \rangle}. \tag{2}$$

where N is the number of atoms in the fullerene, $\langle \cdots \rangle$ denotes a time average, r_{ij} corresponds to the distance between atom i and j.

In principle, for a statistical problem, the studied system is needed to be ergodic, therefore, a long simulation time is commonly needed in MD simulation. In practice, the simulation time is made as long as possible. In Fig.1, we studied the behavior of δ and the temperature's converging as a function of simulation time. It can be

seen that the value of temperature only get well converged after a 50ps simulation, and for δ, even to 100ps, its value doesn't have a good converging behavior to a fine extent. However, the difference between δ calculated in a time scale of 20ps and of 100ps is small (less that 3 percent of the value of 20ps).

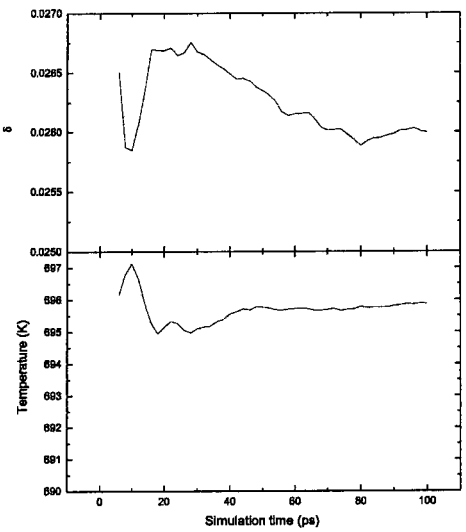

Fig. 1. the converging behavior of the δ and temperature as functions of simulation time in a typical simulation run.

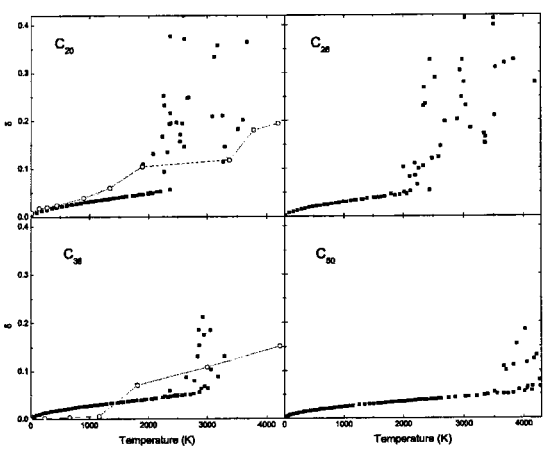

Fig. 2. The δ of fullerene C_{20}, C_{26}, C_{36} and C_{60}, as a function of cluster temperature. The black squares are our current results and the circles in the line are data from ref.2 and 3.

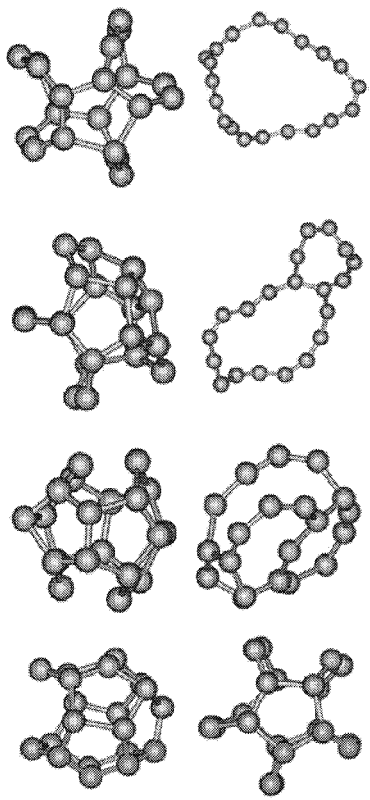

Fig. 3. Some typical isomers of C_{20} formed during the simulation.

3. Results and Discussion

Fig.2 shows the δ values of C_{20}, C_{26}, C_{36} and C_{60} as a function of fullerene temperature. As seen from it, the δ values at low temperatures are low (less than 10%) and continuous, indicating that the fullerene is a solid-like cluster, according to Lindemann criterion. At high temperatures, the δ value becomes scattered points. We find that longer simulation time can not change these scatted points into continuous curve. This phenomenon can be explained as follows: at high temperatures carbon bonds of fullerenes experience more drastic fluctuations than at low temperatures. The fullerene's bonds may break due to some local drastic fluctuation of bonds , therefore the structure changes into an isomer of fullerene. In our simulations, at each fullerene temperature, the starting structure is all the same fullerene cage prepared using thermal quenching technique. Even at the nearly equal temperature, different isomerization transitions may happen due to different local drastic bond length fluctuations. Thus at high temperature, δ values behavior as scattered points. In Fig.3, as an example, different isomers of C_{20} produced during the simulation are shown.

In Fig.3 it can be seen that with the number of atoms of a fullerene cage increases, the discontinuous point of δ happens at a higher temperature, indicating that larger fullerene may be more stable than small one. This is interpreted as the bonding energy per atom of C_{20}, C_{26}, C_{36} and C_{60} are 6.01eV, 6.25eV, 6.45eV and 6.86eV respectively. The C-C bonds are stronger in a larger fullerene cage. On the other hand, in a bigger fullerene cage, the local drastic bond length fluctuations can be buffered because of its neighbor atoms can have larger freedom of motion than in a relatively small cage, therefore their damage to the bonds is buffered.

According to Lindemann's criterion, the melting points (at this temperature the fullerene is undergoing a change from a solid-like to a liquid-like melting transition) of C_{20}, C_{26}, C_{36} and C_{60} are about 1899K, 1998K, 2641K and 3663K. The melting point of C_{20} is quite near to the value from ref.[6], in which it is 1900K. The melting point of C_{36} has a difference of more than 300K, compared with the value of ref.[7]. The circles in Fig.2 show the results of ref.[6] and ref.[7]. It can be seen that for C_{20} the δ is similar to our current result. However, it has no continuous property as our result at the low temperature. This may be due to the inadequacy of simulation steps. For C_{36}, δ in ref.[7] is quite low in the range 0-1500K and the first discontinuous point appears earlier than our result. Because δ is calculated only for a few temperature points especially at high temperature, the tendency of the variation of δ is not fully acquired and the obtained melting point could not reach the better accuracy.

In order to investigate the mechanical stability of C_{20}, we performed a MD simulation of the collision of C_{20} with a graphite (0001) surface. Incident C_{20}'s energy ranges from 10eV to 120eV. The atoms at the fringes of graphite sheets are kept unmoved during the simulation. With an incident energy lower than 15eV, C_{20} will rebound from the graphite surface with the undamaged structure. C_{20} with energy

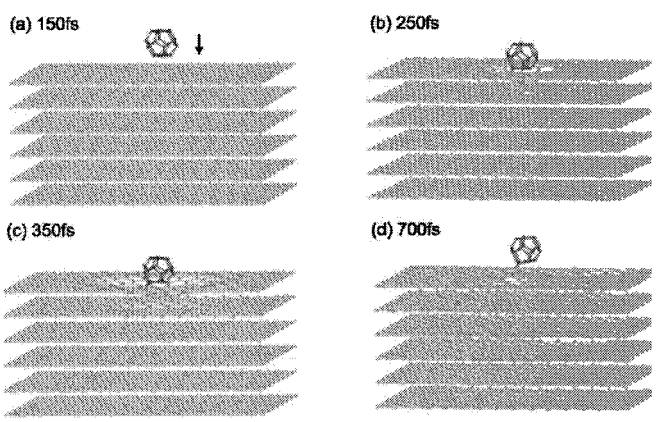

Fig. 4. Snapshots of the C_{20} with incident energy 20eV colliding with a graphite (0001) surface. The initial orientation and position of the C20 is "pentagon down". Fringes of graphite sheets are fixed.

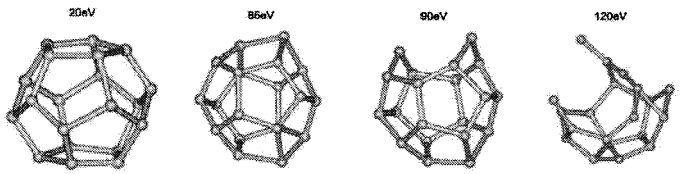

Fig. 5. The structures of C_{20} at the final stage of the collision, with different incident energies.

more than 20eV will collide with graphite surface and the bottom atoms will form bonds with atoms in the graphite surface, which makes the C_{20} cannot escape away from the surface. Fig.4 shows the process of a 20eV C_{20} colliding with the graphite surface. When the incident energy reaches 85eV, the structure after collision is deformed but not broken. Only until 90eV one bond of C_{20} cage break. When the incident energy reaches 120eV, the structure is deformed greatly. Fig.5 show the structures of C_{20} at the final stage of collisions with different incident energy. This result implies that if C_{20} cluster will be a candidate for forming nanostructured films which retain the characteristic properties of the free clusters by means of neutral cluster beam deposition at low energy[10,11], the energy of C_{20} must be smaller than 20eV.

In Ke's work[6], C_{20} are always rebound. It is because of the unphysical nature of the interaction between C_{20} and graphite which is simulated by Lennard-Jones pontential in that work. The atoms of C_{20} will never bond with atoms of graphite in spite of how close they get to each other, because they are in the repulsive range of Lennard -Jones potential as the carbon atoms of C_{20} and graphite get more close.

In summay, the thermal stability of fullerenes is studied using MD simulation. The results show that the rms bond-length fluctuation becomes scattered points at relative high tempereture, which is caused by different isomerization transitions. Larger fullerenes are found to be more stable than small ones. The simulation of C_{20} colliding with graphite shows different results compared with the simulation using TLHT potential in ref.[6]. The present simulation demonstrate that the results obtained from the calculation with Brenner plus L-J potentials seem more reasonable than our previous study.

Acknowledgment

This work is supported by the Key Project of Knowledge Innovation Program of Chinese Academy of Sciences (KJCX2-SW-N02).

References

1. H. W. Kroto, J. R. Heath, S. C. O'Brien, R. F. Curl, R. E. Smalley, *Nature (London)* **318** 162 (1985).
2. T. Takai, C. Lee, T. Halicioglu, and W. A. Tiller, *J. Phys. Chem.* **94** 4480 (1990).
3. J. Tersoff, *Phys. Rev.* **37** 6991 (1988); *Phys. Rev. Lett.* **61** 2879 (1988).

4. D. W. Brenner, O. A. Shenderova1, J. A. Harrison, S. J. Stuart, B. Ni and S. B. Sinnott, *J. Phys.: Condens. Matter* **14** 783 (2002).
5. N. A. Marks, *Phys. Rev. B* **63** 035401 (2000).
6. X. Z. Ke, Z. Y. Zhu, F. S. Zhang, F. Wang, Z. X. Wang, *Chem. Phys. Lett.* **313** 40 (1999).
7. X.Z. Ke, Z. Y. Zhu, F. Wang, F. S. Zhang, Z. X. Wang, *Phys. Lett. A* **255** 294 (1999).
8. P. A. Marcos, J. A. Alonso, A. Rubio, and M. J. Lopez, *Eur. Phys. J. D* **6** 221 (1999).
9. L. A. Girifalco, *J. Phys. Chem.* **96** 858 (1992).
10. V. Paillard, P. Melinon, V. Dupuis, A. Perez, J. P. Perez, G. Guiraud, J. Fomazero, G. Panczer, *Phys. Rev. B* **49** 11433 (1994).
11. V. Paillard, *Phys. Rev. Lett.* **71** 4170 (1993).